



PII S0016-7037(97)00043-4

Dating of the time of sedimentation using U-Pb ages for paleosol calcite

E. T. RASBURY,¹ G. N. HANSON,¹ W. J. MEYERS,¹ and A. H. SALLER²¹Department of Earth and Space Sciences, University at Stony Brook, Stony Brook, New York 11794, USA²UNOCAL Corporation, 14141 Southwest Freeway, Sugar Land, Texas 77478, USA

(Received November 18, 1996; accepted in revised form December 10, 1996)

Abstract—We have sampled paleosol horizons from a continuous core of a rapidly deposited Late Pennsylvanian–Early Permian marine shelf section in Texas, USA. The paleosols occur on the tops of shoaling upward cycles and, based on current time constraints, these cycles average 250 ka and cannot represent longer than 400 ka. As the unconformity which is represented by the paleosol can only be a fraction of the time allowed for deposition of the cycle, the age of minerals that form in the paleosol is effectively the time of sedimentation. The uncertainty on the ^{238}U – ^{206}Pb age of brown paleosol calcite from one exposure surface is only 1 Ma. Reported uncertainties on Paleozoic boundaries are greater than 10 Ma. Our early results suggest that the marine sedimentary record may be dated to a precision of 1 Ma with U-Pb analyses of carefully selected paleosol calcite. These results have implications for vastly improving time resolution of the rock record. Copyright © 1997 Elsevier Science Ltd

1. INTRODUCTION

U-Pb and Pb-Pb ages of carbonates published since the pioneering study of Moorbath et al. (1987) show convincingly that carbonates can be important for dating sedimentary rocks. It is important to identify carbonates that are ubiquitous in the sedimentary record, that are easy to recognize in a well understood geologic framework, that may be inert to later geologic processes, and that form in settings that have a good chance of concentrating uranium. Subaerial exposure surfaces have been shown to have favorable U-Pb systematics (Hoff et al., 1995; Winter and Johnson, 1995); their stratigraphic occurrence is well studied, and the most common carbonate to form in this environment is low Mg calcite (e.g., Esteban and Klappa, 1983). U-Pb dating of soil calcites that formed at exposure surfaces in rapidly deposited cyclic marine sediments (for our purpose the period of sedimentation of one cycle including the time of exposure should be less than one million years) has tremendous potential for directly dating the time of sedimentation. This is because in areas of rapid deposition, the duration of exposure is short so minerals that formed during exposure to meteoric diagenesis and soil processes may record the age of sedimentation.

2. GEOLOGY AND STRATIGRAPHY

An almost continuous drill core through a late Paleozoic sedimentary sequence in the Permian Basin of western Texas, USA (Fig. 1), spans the Pennsylvanian–Permian boundary (290 ± 20 Ma, Harland et al., 1990) which is identified by fusulinid biostratigraphy (UNOCAL core and unpublished biostratigraphy from Garner Wilde). Individual cycles represent about 250 ka based on the assumption that they are quasiperiodic and that the duration of deposition of the strata was ca. 15 Ma, and even considering the uncertainties of the timescale cannot represent more than 400 ka (Saller et al., 1994). Sixty-one cycles are recognized in this core, 25% of which are capped by subaerial exposure surfaces with well-developed soil features including in situ

breccias, nodules, rhizoliths, laminated crusts, and desiccation features such as mud cracks. Brown calcite is commonly associated with these soil fabrics. Our research suggests that uranium may be concentrated in brown paleosol calcite, possibly by organic material. Because petrographic relationships require that the brown calcite is related to soil processes, its age should be the time of subaerial exposure of the specific layer from which it is sampled.

The brown calcite from one soil horizon was used in this study for U-Pb dating. The dated cycle is Early Permian (PW-2-B, near top of Middle Wolfcampian) based on fusulinid biostratigraphy (Wilde, 1990). The paleosol is an in situ breccia and the brecciated interval is more than 30 cm thick. Limestone fragments are displaced like pieces of a puzzle and separated by brown sparry calcite cement (Fig. 2). In hand specimen many (all?) rhizoliths stand out because they are lined by needle fiber calcite which is dark brown. In thin section, the brown calcite has abundant wispy brown-black opaque inclusions of organic residue that are most likely plant remains. A comparison of fission track patterns with cathodoluminescence reveals that uranium is concentrated in the areas of brightest luminescence, associated with needle fiber calcite and flower spar. Needle fiber calcite is low Mg calcite that may occur randomly across pore spaces or tangentially around rhizoliths. It has been interpreted to be the result of fungal activity associated with living roots (Ward, 1975). Based on studies of Recent subaerial exposure surfaces, it is clear that calcification of the fungi is rather rapid (Ward, 1975). Flower spar is also low Mg calcite and in Pleistocene subaerial exposure surfaces of Barbados it is interpreted to form in the fresh water phreatic lens (James, 1972). A summary of the events that are recorded by cement stratigraphy in this rock are (1) dissolution of shells with concomitant filling by coarse mostly nonluminescent but zoned dolomite, (2) paleosol development expressed as rhizoliths that broke up the rock creating the in situ brecciation and the associated brightly luminescent needle fiber calcite and flower spar, (3) molds left by roots are filled by dull

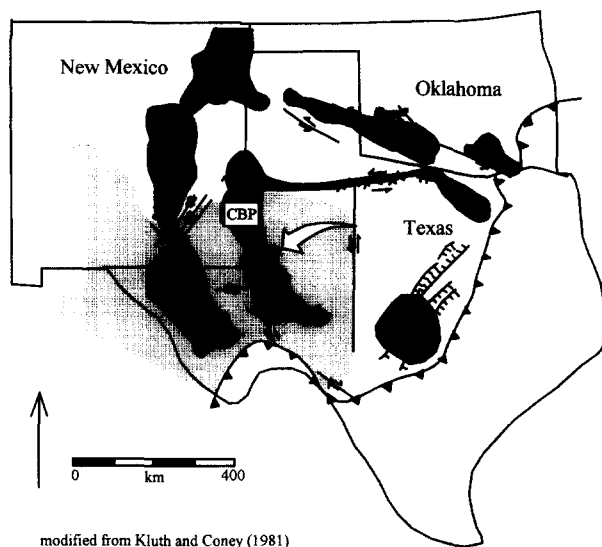


Fig. 1. Map of the southern part of the USA (modified from Kluth and Coney, 1981). The white arrow points to the field where the core used in this study was taken on the Central Basin Platform (CBP) of the Permian Basin. Dark gray areas are Late Paleozoic shelf areas where carbonates accumulated. The light gray area is roughly the Permian, Delaware, and Chihuahua basins from east to west.

luminescent calcite, (4) extensive replacement of the host rock, the early moldic dolomite and the rhizolith filling calcite by a ca. 50 μ dolomite, and (5) 10–20 μ framboidal pyrite which may be concomitant with late dolomite but occurs in all cement types and in some cases particularly lines rhizoliths. The pyrite may provide an important constraint that relates the history of cementation to a time window which includes only subaerial exposure because the pyrite is likely a result of swampy conditions created during the transgression which starts the next cycle (Wright, 1986; Wilkin et al., 1996).

3. SAMPLE SELECTION AND RESULTS

A fragment of the core sample dominated by the brown calcite cement was crushed with a mortar and pestle to coarse sand size fragments. Samples of the darkest brown calcite were hand picked from fractions that were cleaned in acetone and distilled water in a sonicator. The seven samples (20 to 43 mg) that were analyzed for uranium and lead have uranium concentrations from 4.7 to 8.6 ppm, lead concentrations from 0.68 to 0.94 ppm, and the $^{238}\text{U}/^{204}\text{Pb}$ ranges from 532 to 1332 (Table 1).

The unique power of the U-Pb system is that there are two independent isochrons that will give the same age if the system has remained closed to uranium and its daughter products since its formation. The ^{235}U - ^{207}Pb and ^{238}U - ^{206}Pb ages are concordant and give an age for the paleosol of 298 Ma (Fig. 3a, b). However, the uncertainties imposed by the small change in ^{207}Pb make the ^{238}U - ^{206}Pb age the major age constraint (Mattinson, 1987). Therefore, it is worthwhile to consider alternative ways to evaluate the ^{238}U - ^{206}Pb age.

Although the same age information is obtained with any

isochron approach from the same system, isochron plots of the most precise data will provide the most insight into geologic complexities such as initial heterogeneity in the lead isotopes or loss or gain of parent or daughter isotopes.

Because of the two uranium isotopes, ^{238}U and ^{235}U , decaying to two lead isotopes, ^{206}Pb and ^{207}Pb , a number of isochron approaches could be used. In the literature, the $^{238}\text{U}/^{204}\text{Pb}$ - $^{206}\text{Pb}/^{204}\text{Pb}$ isochron has been used almost exclusively to solve for the age of low to intermediate $^{238}\text{U}/^{204}\text{Pb}$ carbonates. The conventional Wetherill (1959) concordia approach has been used for carbonates with high $^{238}\text{U}/^{204}\text{Pb}$. All isochrons require the assumption that the isotopic composition is initially homogenous and that the system has been closed to addition or removal of parent or daughter isotopes throughout the history of the system under investigation. The $^{238}\text{U}/^{207}\text{Pb}$ - $^{206}\text{Pb}/^{207}\text{Pb}$ isochron requires no more assumptions than are made with the $^{238}\text{U}/^{204}\text{Pb}$ - $^{206}\text{Pb}/^{204}\text{Pb}$ isochron. ^{207}Pb changes with the decay of ^{235}U but, because $^{235}\text{U}/^{238}\text{U}$ is assumed to have a constant value since there is no reason to believe that geologic processes would separate these isotopes, no additional assumptions are required. Even if the assumptions required for an isochron are not valid the age calculated with the $^{238}\text{U}/^{207}\text{Pb}$ - $^{206}\text{Pb}/^{207}\text{Pb}$ isochron (or the other two concordia type plots which can also be used as isochrons) will always be identical to the $^{238}\text{U}/^{204}\text{Pb}$ - $^{206}\text{Pb}/^{204}\text{Pb}$ isochron.

The $^{206}\text{Pb}/^{207}\text{Pb}$ measurements have lower analytical uncertainties than $^{206}\text{Pb}/^{204}\text{Pb}$ because ^{207}Pb is at least 15 times as abundant as ^{204}Pb and therefore ^{207}Pb is always measured more easily. In the example presented here, the $^{238}\text{U}/^{207}\text{Pb}$ has the same uncertainty as the $^{238}\text{U}/^{204}\text{Pb}$ because of the uncertainty in the ^{205}Pb measurement for Pb concentration is as great as that for ^{204}Pb (Table 1).

When the data are plotted on the $^{238}\text{U}/^{204}\text{Pb}$ - $^{206}\text{Pb}/^{204}\text{Pb}$



Fig. 2. Contrast enhanced computer scanned image of a polished slab of the rock from which the U-Pb data in this paper come. The area scanned is 4 \times 5 cm². (a) is the original limestone and fragments of the same all of which are extensively dolomitized; (b) dark brown calcite that is needle fiber calcite and flower spar and is where uranium is concentrated in this sample; (c) incipient brecciation of the host carbonate by rhizoliths.

Table 1. Data from brown paleosol calcite from a UNOCAL core of the Pennsylvanian-Early Permian section of the Central Basin Platform of the Permian Basin of West Texas. All ratios are blank and fractionation corrected except $^{205}\text{Pb}/^{206}\text{Pb}$.

	wt (mg)	Pb ppm	U ppm	$^{238}\text{U}/$ ^{204}Pb	2s %	$^{235}\text{U}/$ ^{207}Pb	2s %	$^{206}\text{Pb}/$ ^{204}Pb	2s %	$^{207}\text{Pb}/$ ^{206}Pb	2s %	$^{208}\text{Pb}/$ ^{206}Pb	2s %	$^{205}\text{Pb}/$ ^{206}Pb	2s %
x-1-1a	42.66	0.68	5.8	872	0.4	0.3541	0.4	61.234	0.2	0.29168	0.1	0.63452	0.2	0.013446	0.2
x-1-1b	26.50	0.8	7.3	941	0.4	0.3786	0.3	64.573	0.2	0.27921	0.1	0.60213	0.2	0.009074	0.1
x-1-1e	26.45	0.69	7.5	1332	0.4	0.5094	0.3	83.006	0.3	0.22845	0.2	0.46643	0.3	0.013558	0.1
x-1-1g	19.34	0.95	8.6	969	0.5	0.3869	0.3	65.919	0.3	0.2755	0.2	0.58863	0.2	0.006737	0.4
x-1-1c	32.82	0.71	7.1	1152	0.5	0.4508	0.3	74.691	0.2	0.24861	0.2	0.51939	0.2	0.008838	0.2
x-1-1d	24.98	0.78	4.7	532	0.3	0.2272	0.3	45.206	0.2	0.37576	0.1	0.85230	0.2	0.010574	0.2
x-1-1f	20.60	0.70	7.5	1279	0.5	0.4918	0.5	80.825	0.3	0.23333	0.3	0.48065	0.3	0.007985	0.3

isochron the MSWD of the line is 1.48 (Table 2, Fig. 3a), whereas the MSWD of the $^{238}\text{U}/^{207}\text{Pb}$ - $^{206}\text{Pb}/^{207}\text{Pb}$ isochron is 0.9 (Table 2, Fig. 3c) even though the uncertainties on the analyses of $^{206}\text{Pb}/^{204}\text{Pb}$ are greater than or equal to the

uncertainty in the $^{206}\text{Pb}/^{207}\text{Pb}$ measurements in every case. The lower MSWD could result from random statistics of the small dataset, but we have compared results from a number of datasets generated at Stony Brook and in most cases the

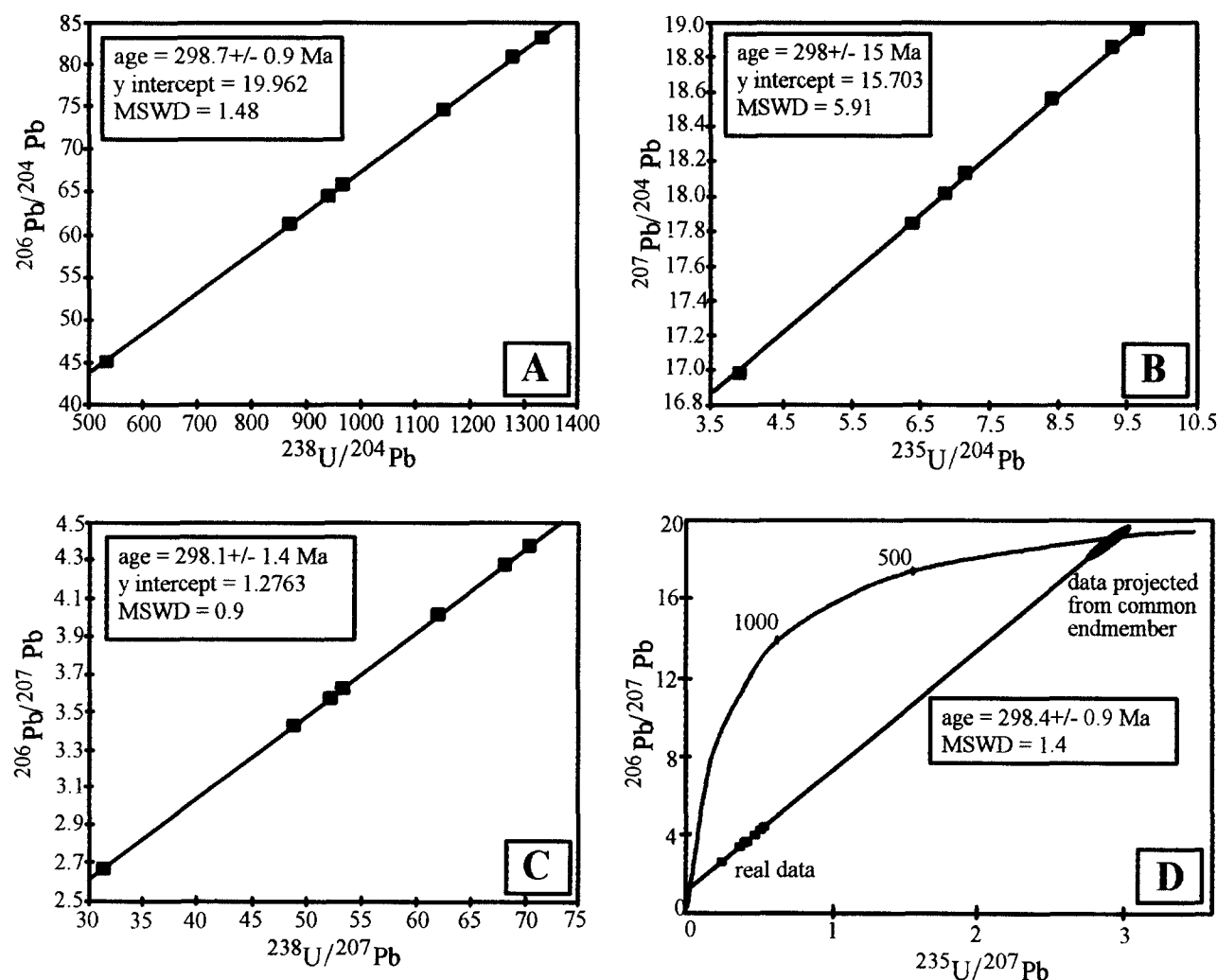


Fig. 3. U-Pb isochrons for brown calcite from an Early Permian in situ brecciated limestone. (a) The $^{238}\text{U}/^{204}\text{Pb}$ - $^{206}\text{Pb}/^{204}\text{Pb}$ isochron is used most often for carbonate data. (b) The $^{235}\text{U}/^{204}\text{Pb}$ - $^{207}\text{Pb}/^{204}\text{Pb}$ isochron provides a check for the $^{238}\text{U}/^{204}\text{Pb}$ - $^{206}\text{Pb}/^{204}\text{Pb}$ isochron. (c) The $^{238}\text{U}/^{207}\text{Pb}$ - $^{206}\text{Pb}/^{207}\text{Pb}$ isochron provides the same age as the standard $^{238}\text{U}/^{204}\text{Pb}$ - $^{206}\text{Pb}/^{204}\text{Pb}$ isochron and the MSWD is smaller. (d) The 3-dimensional concordia plot is a projection from the common lead plane onto the concordia plane. The ellipse that falls on concordia is the uncertainty on the isochron projection. Individual points plot inside this ellipse and have much smaller uncertainties.

Table 2. Ages calculated from seven analyses of brown paleosol calcite using the ISOPLOT program of Ludwig (1994) for various isochrons, and K. R. Ludwig (pers. commun. for the 3-d approach).

isochron used	age (Ma)	uncertainty (Ma)	MSWD	figure
$^{238}\text{U}/^{204}\text{Pb}$ — $^{206}\text{Pb}/^{204}\text{Pb}$	298.7	0.9	1.48	3a
$^{235}\text{U}/^{204}\text{Pb}$ — $^{207}\text{Pb}/^{204}\text{Pb}$	298	15	5.91	3b
$^{207}\text{Pb}/^{204}\text{Pb}$ — $^{206}\text{Pb}/^{204}\text{Pb}$	289	130	4.2	not shown
$^{238}\text{U}/^{207}\text{Pb}$ — $^{206}\text{Pb}/^{207}\text{Pb}$	298.1	1.4	0.9	3c
$^{204}\text{Pb}/^{207}\text{Pb}$ — $^{206}\text{Pb}/^{207}\text{Pb}$ — $^{235}\text{U}/^{207}\text{Pb}$	298.4	0.9	1.4	3d

MSWD (and usually the age uncertainty) is lower with the $^{238}\text{U}/^{207}\text{Pb}$ — $^{206}\text{Pb}/^{207}\text{Pb}$ isochron. Because the percent spread in the data is identical for the two systems there must generally be more initial heterogeneity in $^{206}\text{Pb}/^{204}\text{Pb}$ than in $^{207}\text{Pb}/^{206}\text{Pb}$, because otherwise the MSWD of the data with the greater uncertainties would be lower.

The data may also be viewed on a three-dimensional concordia plot where they are projected onto the two-dimensional concordia plot from a common lead endmember (Fig. 3d). The precision of the age is not limited by the uncertainty in the ^{204}Pb measurement if the regression algorithm weights the points by their X-Y-Z errors and error correlations (Ludwig and Titterton, 1994). Data plotted in this way lie on concordia and the uncertainty in the age and the MSWD are similar to that for the $^{238}\text{U}/^{204}\text{Pb}$ — $^{206}\text{Pb}/^{204}\text{Pb}$ isochron (K. R. Ludwig, pers. commun.). This approach requires measurement of ^{204}Pb and in some cases this is difficult to achieve even when the $^{207}\text{Pb}/^{206}\text{Pb}$ can be measured precisely.

The $^{238}\text{U}/^{207}\text{Pb}$ — $^{206}\text{Pb}/^{207}\text{Pb}$ isochron has been used as a concordia type plot for the lunar rocks where common lead was subtracted (Tatsumoto, 1972), as a three-dimensional concordia plot as used here (Fig. 3d; Zhang, 1990) and as an isochron where ^{207}Pb is assumed not to change (Getty and DePaolo, 1995; and also see their derivation of the isochron equation where ^{207}Pb is allowed to change as used here) but otherwise has been generally overlooked in dating other rocks. This approach is not different than the other two concordia plots of Wetherill (1959) and Tera and Wasserburg (1972) which will give identical isochron ages and all are the ^{238}U — ^{206}Pb age. We choose the Tatsumoto (1972) plot because it has lower error correlations than the Wetherill (1959) plot and has a positive slope unlike the Tera and Wasserburg (1972) plot. An important point here is that we are not assuming concordance. We do not subtract common lead, we use data that is only corrected for blank and fractionation. The line is an isochron representing the mixing between common initial lead and radiogenic lead produced since the calcite was deposited.

The three-dimensional approach is appealing because it is easy to see by inspection that the data are concordant, but this approach provides no additional information than may be gleaned from the ^{238}U — ^{206}Pb isochrons and the ^{235}U — ^{207}Pb isochron. With very precise analyses and a MSWD of 0.9 there is little suggestion of geologic complexity in the U-Pb system and we have a high degree of confidence that we know the age of this exposure surface to within 1.4 Ma.

4. IMPLICATIONS FOR THE PENNSYLVANIAN-PERMIAN BOUNDARY

The Carboniferous-Permian boundary is considered to be 290 ± 20 (Harland et al., 1990) or 295 ± 5 (Ross et al., 1995). The Carboniferous-Permian boundary is approximately 2 Ma younger than the Pennsylvanian-Permian boundary (Wilde, 1990). These ages are indistinguishable from the cycle top age of 298.1 ± 1.4 Ma. However, the age reported here is from a cycle top that is almost 100 m above the Pennsylvanian-Permian boundary as identified by fusulinid biostratigraphy (UNOCAL, unpubl. data), and it should be several million years younger than the boundary.

5. CONCLUSIONS

Because the duration of exposure of rapidly deposited cyclic marine sediments is much less than a million years (the precision of the dating) and these surfaces occur on the scale of meters, calcites that formed at those surfaces have great potential for directly dating the time of sedimentation. The ^{238}U — ^{206}Pb age of soil-formed brown calcite occurring on an Early Permian cycle-capping subaerial exposure surface is 298.1 ± 1.4 Ma. Cycles like the one dated are reported from rocks throughout the Phanerozoic (Esteban and Klappa, 1983). Our results suggest that the marine sedimentary record could conceivably be dated to a precision of a million years by careful evaluation of the relative time relationships and sampling carbonate components that effectively record the time of sedimentation.

Although the same age information is obtained with any isochron approach from the same system, isochron plots of the most precise data will provide the most insight into geologic complexities. For this reason, the $^{238}\text{U}/^{207}\text{Pb}$ — $^{206}\text{Pb}/^{207}\text{Pb}$ isochron or a three-dimensional concordia approach have advantages over the more commonly used $^{238}\text{U}/^{204}\text{Pb}$ — $^{206}\text{Pb}/^{204}\text{Pb}$ isochron.

Acknowledgments—Funding for the project was provided by a Department of Energy grant to G.N. Hanson and W.J. Meyers. J.A.D. Dickson helped with sampling the core. S. Hemming is especially thanked for help with the $^{238}\text{U}/^{207}\text{Pb}$ — $^{206}\text{Pb}/^{207}\text{Pb}$ isochron. We thank K. Mezger, S. Hemming, G. Hemming, V. Pedone, S. McLennan, P. Bliefus, R.L. Folk, and B. Ward for reviewing earlier drafts of the manuscript. Discussions with B. Ward, A. Lanzirrotti, F. Marcantonio, S. Carr, P. Tomascak, and K. Ludwig were also very helpful.

REFERENCES

- Esteban M. And Klappa C. F. (1983) Subaerial exposure environment. In *Carbonate Depositional Environments* (ed. P. A. Scholle et al.); *AAPG Mem.* **33**, 1–54.
- Getty S. R. and DePaolo D. J. (1995) Quaternary geochronology using the U-Th-Pb method. *Geochim. Cosmochim. Acta* **59**, 3267–3272.
- Harland W. B., Armstrong R. L., Cox A. L., Craig L. E., Smith A. G., and Smith D. G. (1990) *A Geologic Time Scale 1989*. Cambridge University Press.
- Hoff J. A., Jameson J., and Hanson G. N. (1995) Application of Pb isotopes to the absolute timing of regional exposure events in carbonate rocks: An example from U-rich dolostones from the Wahoo Formation (Pennsylvanian), Prudhoe Bay, Alaska. *J. Sediment. Res.* **A65**, 225–233.
- James N. P. (1972) Holocene and Pleistocene calcareous crust (caliche) profiles: Criteria for subaerial exposure. *J. Sediment. Petrol.* **42**, 817–836.
- Kluth C. F. and Coney P. J. (1981) Plate tectonics of the Ancestral Rocky Mountains. *Geology* **9**, 10–15.
- Ludwig K. R. (1994) *Isoplot. Version 2.71. USGS Open-File Report 91–445*.
- Ludwig K. R. and Titterton D. M. (1994) Calculation of $^{230}\text{Th}/\text{U}$ isochrons, ages, and errors. *Geochim. Cosmochim. Acta* **58**, 5031–5042.
- Mattinson J. M. (1987) U-Pb ages of zircons: A basic examination of error propagation. *Chem. Geol.* **66**, 151–162.
- Moorbath S., Taylor P. N., Orpen J. L., Treloar P., and Wilson J. F. (1987) First direct radiometric dating of Archean stromatolitic limestone. *Nature* **326**, 865–867.
- Ross C. A., Baud A. Menning M. (1995) A time scale for project Pangea. *Canadian Soc. Petrol. Geol. Mem.* **17**, 81–83.
- Saller A. H., Dickson J. A. D., and Boyd S. A. (1994) Cycle stratigraphy and porosity in Pennsylvanian and Lower Permian shelf limestones, eastern Central Basin Platform, Texas. *AAPG Bull.* **78–12**, 1820.
- Tatsumoto M., Hedge C. E., Doe B. R., and Unruh D. M. (1972) U-Th-Pb and Rb-Sr measurements on some Apollo 14 lunar samples. *Proc. 3rd Lunar Conf. (Suppl. 3, Geochim. Cosmochim. Acta)* **2**, 1531–1555.
- Tera F. And Wasserburg G. J. (1972) U-Th-Pb systematics in three Apollo 14 basalts and the problem of initial Pb in lunar rocks. *Earth Planet. Sci. Lett.* **14**, 281–304.
- Ward W. C. (1975) Petrology and diagenesis of carbonate eolionites of northeastern Yucatan Peninsula, Mexico. In *Studies in Geology No. 2* (ed. K. F. Wentland and W. C. Pusey III), pp. 500–571. AAPG.
- Wetherill (1959) Discordant uranium-lead ages, I. *Trans. AGU* **37**, 320–326.
- Wilde G. L. (1990) Practical fusulinid zonation: The species concept; with Permian Basin emphasis. *West Texas Geol. Soc. Bull.* **29–7**, 5–34.
- Wilkin R. T., Barnes H. L., and Brantley S. L. (1996) The size distribution of framboidal pyrite in modern sediments: An indicator of redox conditions. *Geochim. Cosmochim. Acta* **60**, 3897–3912.
- Winter B. L. and C. M. Johnson (1995) U-Pb dating of carbonate subaerial exposure event. *Earth Planet. Sci. Lett.* **131** 177–187.
- Wright V. P. (1986) Pyrite formation and the drowning of a palaeosol. *Geol. J.* **21**, 139–149.
- Zhang Y.-F. (1990) A further three-dimensional U-Pb method for solving the two-stage episodic model. *Geochem. J.* **24**, 29–37.